Tribol Lett (2015) 59:29
DOI 10.1007/s11249-015-0557-7

ORIGINAL PAPER

An Oil-Based Lubrication System Based on Nanoparticular TiO_2 with Superior Friction and Wear Properties

Lukas Bogunovic[1] · Sebastian Zuenkeler[1] · Katja Toensing[1] · Dario Anselmetti[1]

Received: 19 March 2015 / Accepted: 9 June 2015 / Published online: 21 June 2015

Abstract We evaluated the performance of five different commercially available nanoparticle classes as additives for an oil-based lubrication system. While the silicon dioxide particles Aerosil® 300, RY300, and R972V tended to increase wear and friction in our 100Cr6 versus cast iron disc–disc contact, Aeroxide® P 25 and especially T 805 TiO_2 nanoparticles showed superior anti-wear *and* anti-friction properties. The underlying tribological mechanism was investigated with optical microscopy, helium ion microscopy, and X-ray photoelectron spectroscopy. Subsequently, we formulated a stable lubrication system based on the best performing T 805 particles. Here, the base oil is a highly purified paraffin oil which was supplemented with 1 wt% T 805 TiO_2 particles, 1 wt% Estisol® 242 or 1 wt% oleic acid, 0.15 wt% oleylamine, and 0.15 wt% Pluronic® RPE 2520. Superior lubrication and anti-wear properties of this formulation were demonstrated in 4-h test runs with a normal force of $F_N = 2.5$ kN and a sliding velocity of 0.15 m/s in our disc–disc contact. Wear was significantly reduced along with a nearly 12-fold reduction in the friction coefficient, compared to the base oil ($\mu^{\text{fto}}_{\text{base}} = 0.155$ vs. $\mu^{\text{fto}}_{\text{T805}} \approx 0.01$). Using 100Cr6 disc–ball contacts, we additionally analyzed the properties of our lubrication system in the border friction regime under higher loads ($F_N = 0.5$ kN) in 2-h runs. In particular, on the discs with lower engagement ratio, chemo-tribological protective layers were built, which protected the parts very well against wear.

Keywords Nanoparticle additives · Titanium dioxide · Friction · Wear · Lubrication · Dispersion

1 Introduction

In contrast to conventional solid-state lubricants, the additivation with nanoparticles not only facilitates the production of stable suspensions but also guarantees, especially when parts with low surface roughness are in use, that particles will intrude quickly into the surface contact zone and create a protective layer. Besides the simple particle size reduction in conventional solid-state lubricants such as graphite, molybdenum disulfide, or tungsten disulfide to the nanoscale, the use of silicon dioxide [1, 2], lanthanum borate [3], zinc oxide [4], copper [5–7], calcium carbonate [8], lead sulfide [9], and titanium dioxide [10–12] nanoparticles led to remarkable wear and friction properties of lubricating agents. Another interesting approach are fullerenes. Because of their inherently enclosed form without boundaries or edges, they do not provide reactive bindings sites and elastically roll very nicely into the contact zones [13–15]. In this work, we analyze the suitability of seven different industrially available and reasonably priced SiO_2 and TiO_2 nanoparticles as additive for an oil-based lubricant. Based on the best performing type, we present a recipe for a superiorly formulated lubrication system with long shelf time and analyze it concerning friction and wear in 100Cr6 versus cast iron disc–disc and 100Cr6 disc–ball contacts.

Electronic supplementary material The online version of this article (doi:10.1007/s11249-015-0557-7) contains supplementary material, which is available to authorized users.

✉ Lukas Bogunovic
bogunovic@physik.uni-bielefeld.de

[1] Experimental Biophysics and Applied Nanoscience, Faculty of Physics, Bielefeld Institute for Biophysics and Nanoscience (BINAS), Bielefeld University, Universitaetsstrasse 25, 33613 Bielefeld, Germany

2 Materials and Methods

2.1 Experimental Setup

All results in this work were obtained with the rotation tribometer RT8000, developed, and manufactured at the competence center for tribology at HS Mannheim, Germany. It is actuated with the servo motor MCS12L41 (Lenze SE, Germany) with $p = 4.7$ kW and a rated speed of 4050 rpm. Normal loads up to 10 kN can be exerted on a tribocontact with a pneumatic cylinder which is actuated with a R414002402 pressure-regulating valve (Bosch Rexroth, Germany). A two-component force sensor (Lorenz Messtechnik, Germany) constantly measures the applied normal force F_N and the resulting friction moment M_R. To monitor wear, the touch probe DG/2.5 (Solartron Metrology, UK) is used. Temperature measurements were taken with type K sensors. Data acquisition was done with the provided LabView-based control software "RT8000 control."

2.2 Preparation of Disc–Disc and Disc–Ball Tribocontacts

Our tribology studies were conducted with disc–disc (Fig. 1a) and disc–ball contacts (Fig. 1b). The disc–disc contacts consist of segmented homemade cast iron discs based on [16] (Fig. 1c) and 100Cr6 axial bearing discs (LS2542, Schaeffler, Germany, Fig. 1d). To realize perfectly planar disc surfaces, both parts were lapped before with a Wesentzky-3R55GR lapping machine (Peter Wolters, Germany) for 30 min at 30 rpm with a normal force of 4.5 N. For this purpose, the lapping oil OL 20 Plus and silicon carbide particles (grain 800, 100 g per liter oil) were used (both from Stähli Läpp Technik, Switzerland). After the lapping process, both discs were cleaned in a 1:1 mixture of acetone and petroleum ether in an ultrasonic bath for 2 min. Silicon carbide residues were removed with a K4-10 CO_2 snow cleaner (Applied surface technologies, USA) just before assembly.

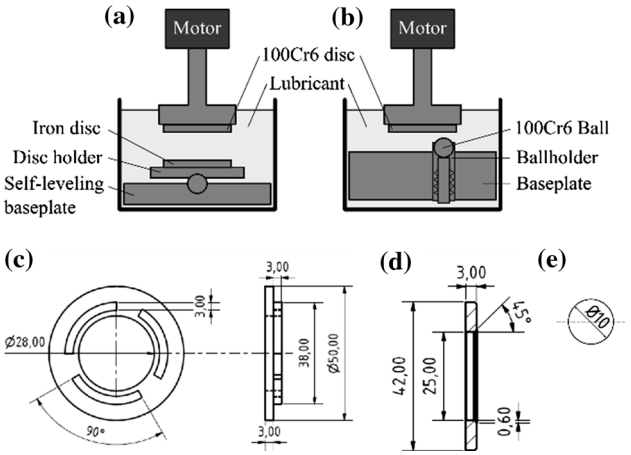

Fig. 1 In the present study, we used 100Cr6 disc versus cast iron disc contacts to evaluate friction coefficients (**a**) and 100Cr6 ball versus disc contacts (**b**) to measure the anti-wear performance of our lubricants. **c** Drawing of the segmented cast iron disc (total active area: 247 mm^2). **d** Drawing of the LS2542 100Cr6 axial bearing disc. **e** Drawing of the 100Cr6 ball. All discs were lapped before use to generate planar surfaces

The disc–ball contacts consist of the same 100Cr6 axial bearing discs and 100Cr6 balls (grade G28, Spherotech Germany, Fig. 1e). The discs were prepared as described above, while the balls were cleaned for 2 min in an ultrasonic bath in a 50:50 mixture of acetone and petroleum ether only.

We performed our tribological investigations with the following parameters. The probe pot containing the tribocontact was filled with lubricant, making sure that all involved parts were properly covered (approximately 200 ml). We chose the following test protocol for the disc–disc contact. In the first 10 s, the rotation speed was increased linearly from zero to $v = 0.15$ ms^{-1} and kept at this value throughout the whole experiment. Subsequently, we increased the normal load every 5 min by 250 N until the maximum load of 2500 N was reached. After this start-up phase, we kept the normal load at 2500 N for 3 h. The disc–ball protocol is different. During the first 10 s, the velocity was increased from zero to 0.5 m/s and kept constant for the rest of the run. We subsequently increased the force every 5 min by 100 N until the maximum load of 500 N was reached. The parameters were kept constant for two further hours.

2.3 Formulation of Nanolubricants

Food-tech-oil (Bio-Circle Surface Technology, Germany) is a H1-certified paraffin oil and serves as basis for all lubricants in this work. Our best performing formulation for a TiO_2 nanoparticle-based lubricant provides the following additives: 1 wt% Aeroxide® T805 TiO_2 nanoparticles (Evonik Industries, Germany), 15 wt% technical oleylamine (Sigma-Aldrich, USA), 15 wt% Pluronic® RPE 2520 (BASF, Germany), and 100 wt% Estisol® 242 (Dow Chemical, USA). All concentrations are referenced to the nanoparticle concentration, except for the nanoparticle concentration itself, which is referenced to the amount of base oil. Alternative formulations are defined in the text. The lubricant was produced by mixing all ingredients with 100 ml of the base oil. Subsequently, the mixture was homogenized in a 100-ml glass flask with a SONOPLUS HD 3200 apparatus ($p_{US} = 200$ W, $\Delta t = 2$ min, $v = 20$ kHz, Bandelin electronic, Germany) in combination with a VS 70 T sonotrode (Ø = 13 mm). To dissipate

heat, the bottle was cooled with an ice bath during the procedure. Finally, we diluted the dispersion with food-tech-oil to the desired final concentration, homogenized it again, and stored it afterward. The lubricant was treated with ultrasound for 2 min again just before use.

3 Results and Discussion

To perform reproducible and comparable tribological investigations with disc–disc contacts, special attention must be paid to disc surface characteristics. When considering the Stribeck curve, it is clear that the mean surface roughness has an important impact on friction and wear. Besides surface roughness, the actual surface geometry plays an important role in the formation of lubricating films between the tribopartners as well [17]. In particular, high demands are made on the planarity of the test pieces to equally distribute the normal load on their whole surface. These requirements are almost ideally met by our lapping procedure. It allows for the preparation of surfaces with low skew and kurtosis and especially with nearly equal mean roughness R_a, which is determined by the choice of the SiC grain size (Fig. 2). Due to the steady change in polishing directions, no preferred abrasion directions were observable, which could systematically alter the lubrication mechanisms while we achieved a high degree of planarity.

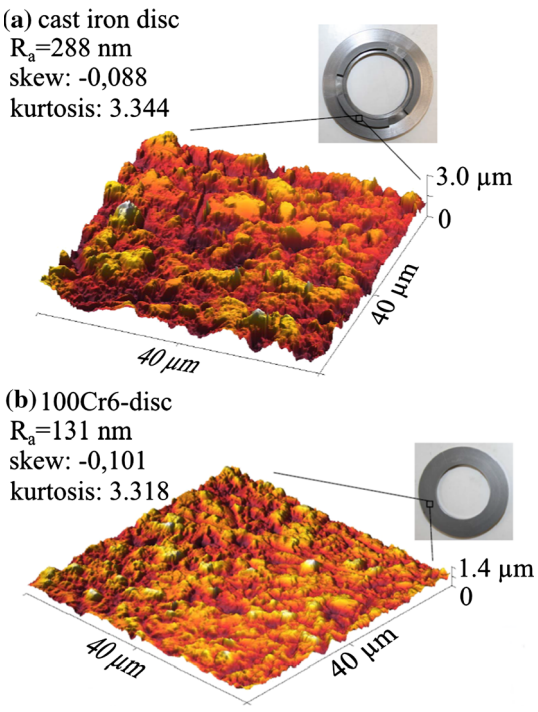

Fig. 2 Photographs of the two discs that make up the tribocontact in this work and their surface parameters after lapping, obtained via 40 × 40 µm^2 atomic force microscopy scans (Color figure online)

Using disc–disc contacts (Fig. 1a), we first addressed the friction coefficient. To judge the influence of our proposed lubrication additives, we conducted negative control experiments to analyze the friction coefficient of the plain base oil. With a falling ball viscometer, we determined dynamic viscosities of $\eta^{\text{fto}}_{20\,^\circ\text{C}} = 198$ m Pa s and $\eta^{\text{fto}}_{40\,^\circ\text{C}} = 65.5$ m Pa s at a density of $\rho^{\text{fto}}_{20\,^\circ\text{C}} = 0.88$ kg l^{-1}. Using only the base oil, we obtained the results shown in Fig. 3. After an initial value of approximately $\mu^{\text{fto}}_{\text{base}} = 0.05$, the friction coefficient increases stepwise with the increasing applied normal load during the start-up phase. This behavior is consistent with the Stribeck function and reveals that the systems operate at the border of mixed friction and boundary friction while the latter is more and more predominant with time. After the initial start-up phase, the friction coefficient is nearly constant at $\mu^{\text{fto}}_{\text{base}} = 0.115 \pm 0.0085$ with slight high-pitched acoustic emissions from time to time. During the experiment, the oil temperature increases from room temperature to approximately 90–100 °C (see Sect. 1 of the supplementary information). In this condition, the system starts to operate in the boundary friction regime, where the surfaces are only separated from each other by a very small amount of lubricant. The reduction in the lubrication film thickness leads at first to an increase in viscosity and for very thin films to a transition into a solid-like condition of the lubricant. Consequently, the change in viscosity with temperature does not play an important role anymore. The actual material combination is more relevant [18, 19].

We inspected the wear mechanisms during the experiment with optical microscopy (Fig. 4). The 100Cr6 discs (Fig. 4a, b) were just smoothed out to $R_a = 25.0$ nm (see exemplary AFM measurement of a 100Cr6-disc in Fig. 2 of the supplementary information). On the other hand, the cast iron disc shows significant wear. Scars in the direction

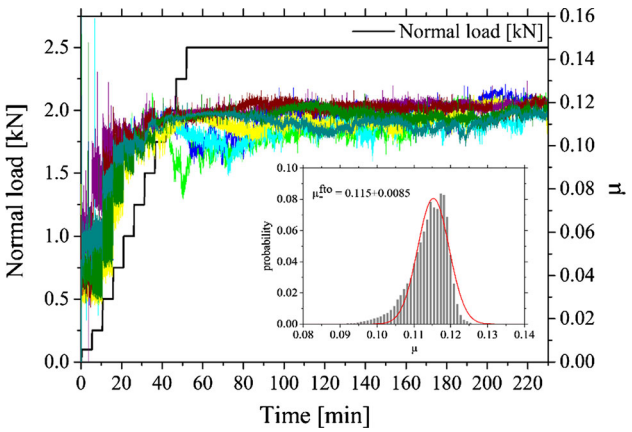

Fig. 3 Friction coefficients of 100Cr6 versus cast iron contacts. Lubrication: food-tech-oil without additives (Color figure online)

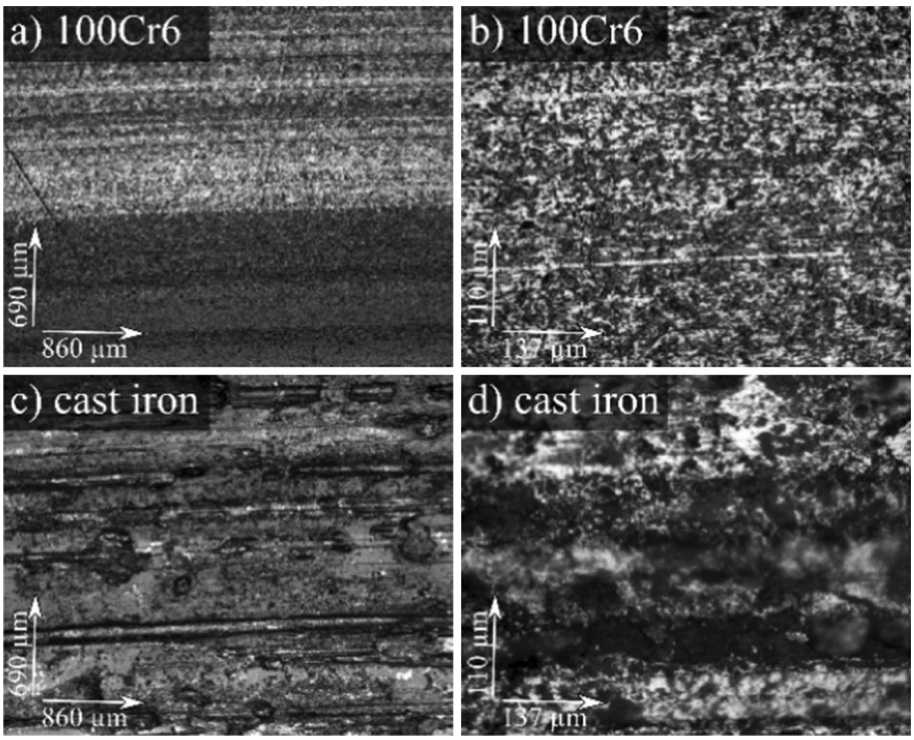

Fig. 4 Optical micrographs showing running marks on (**a**), (**b**) an exemplary 100Cr6-disc and (**c**), (**d**) its corresponding cast iron counterpart after a tribometric study with plain food-tech-oil

of movement demonstrate massive abrasion while surface disruptions hint at adhesive wear as well. One can conclude from the slight brownish staining of the oil during the experiment that also tribochemical reactions took place, which benefit from the high oil temperatures and very thin lubricating films [20].

3.1 Optimization of Friction Coefficients with a Disc–Disc Contact

To overcome these serious limitations of the previous test runs, we used different types of nanoparticles as main oil additives to realize a stable lubricant with superior anti-wear properties *and* lower friction coefficients. Our materials of choice were titanium dioxide and silicon dioxide (Table 1). The five different particle types are commercially available in large quantity at reasonable prices.

Figure 5 shows exemplary realizations of disc–disc experiments with the three different types of silicon oxide particles (blue graphs) and the two different titanium oxide variants (green graphs) each with 0.2 wt% concentration in the base oil. When SiO_2 particles are used as additive, one can conclude from the steadily rising friction coefficients throughout the measurement that these particles tend to destroy the protecting oxide or adhesion layers on the disc surfaces. Total part failures of the tribosystem were the consequence, which occurred within 1 h after the full normal load was reached.

The experiments with titanium dioxide look more promising. From Fig. 5, it can be discerned that T 805 particles cause a reduction in the friction coefficient during

Table 1 Properties of the employed nanoparticles

Product	Aerosil® 300	Aerosil® RY 300	Aerosil® R 972V	Aeroxide® P 25	Aeroxide® T 805
Material	SiO_2	SiO_2	SiO_2	TiO_2	TiO_2
Surface (m^2/g)	300 ± 30	110–140	110 ± 20	50 ± 15	45 ± 10
Size (nm)	7	7	16	21	21
Tapped density (g/l)	50	40	90	130	200
pH (4 % suspension)	3.7–4.7	4.5–5.5	3.4–4.4	3.5–4.5	3.0–4.0
Surface modification		Silicone oil	Dimethyldichlorosilane		Octylsilane

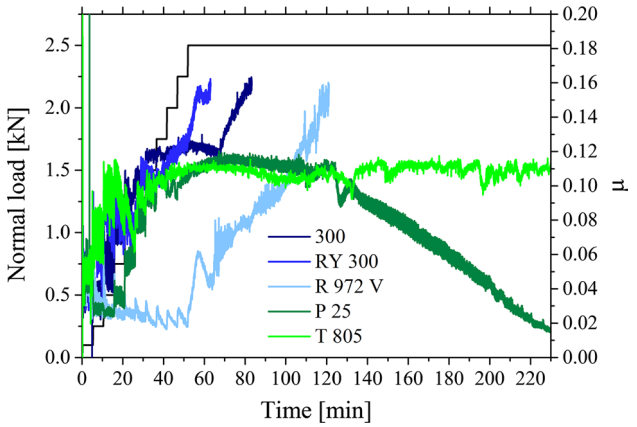

Fig. 5 Exemplary tribostudies with our disc–disc contact and food-tech-oil, supplemented with 0.2 wt% of the SiO_2 particles Aerosil® A300, RY300 or R972 V (blueish), or Aeroxide® TiO_2 particles P 25 or T 805 (*greenish*), respectively, with no further additives. All SiO_2 particle mixtures established an insufficient lubrication film resulting in quick device failure within 1 h after the full load was reached. However, the TiO_2 particles performed similar to the plain base oil or better (Color figure online)

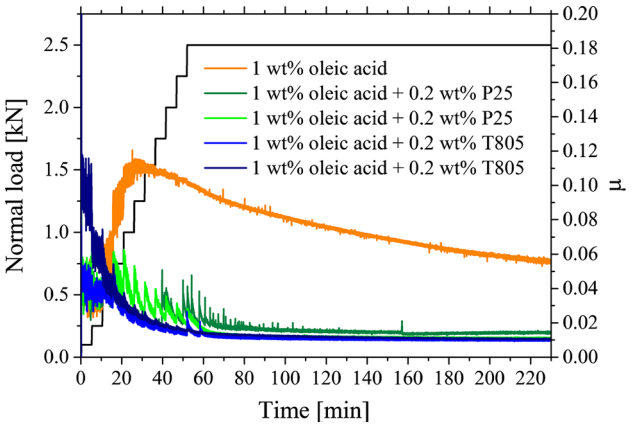

Fig. 6 Disc–disc triboexperiments based on food-tech-oil with 1 wt% oleic acid as negative control (orange) and with 1 wt% oleic acid +0.2 wt% of P 25 (*greenish*) or T 805 (*blueish*) titanium dioxide nanoparticles, respectively. Addition of titanium dioxide nanoparticles leads to a significant and stable reduction in friction coefficients. Mean friction coefficients for the P 25 particles are $\mu_{P25}^{fto} = 0.015 \pm 0.002$ and $\mu_{P25}^{fto} = 0.012 \pm 0.001$, respectively. Friction coefficients of T 805 are slightly lower with $\mu_{T805}^{fto} = 0.010 \pm 0.001$ and $\mu_{T805}^{fto} = 0.016 \pm 0.001$ and therefore significantly smaller than the negative control (Color figure online)

the start-up phase, although the normal load is further increased. However, after the start-up phase, the friction coefficient returns to values comparable to non-supplemented base oil. P 25 particles on the other hand were able to build up a stable lubricating film between the discs and thus lead to significantly lower friction coefficients. However, the full reduction in friction required several hours to establish and was somewhat unstable as can be seen at several time points.

In order to control the built-up of a stable lubrication film with titanium dioxide nanoparticles, to reduce the start-up time and to formulate a stable suspension, further synergetic surfactants were required. A positive influence on the friction properties and the dispersibility in oil can be induced by surface modification of the particles, e.g., with stearic [21] or oleic acid [22]. However, we did not consider a synthesis of particles with such a surface modification because of economic reasons. A simple addition of stearic acid was not possible as well, as it does not form stable suspensions in oil. However, oleic acid is very well soluble in oil. When used in 1 wt% concentration in the base oil, it reduces the friction coefficient slowly from 0.115 to approximately 0.06 (Fig. 6). When adding P 25 and T 805 particles to the solution, the full influence of the particles and the oleic acid becomes apparent immediately after the experiment was started. This effect seems to be synergetic, especially for the hydrophobic T 805 particles. Without oleic acid, friction coefficients are roughly unchanged compared to the pure base oil (Fig. 5). In contrast, Fig. 6 shows a significant reduction in friction when oleic acid is combined with T 805 particles especially when compared to the values for oleic acid alone. The mixtures observably establish a stable lubricating film, leading to very low friction coefficients smaller than 0.016 with 2.5 kN (10 MPa) normal load in our disc–disc contact. Under these conditions, P 25 and T 805 particles show similar properties and were considered further.

The nanoparticles develop their full potential, when the tribocontact operates in the mixed friction regime. While there are still some material collisions present, the particles can fill the gaps in between and carry a fraction of the applied load, thus averting material contacts [23]. Elastic and plastic deformations due to shear forces are thus partly transferred from the tribopartners to the nanoparticles [24]. The gradually smoothing of the surfaces and the ability of the particles to transfer pure sliding friction into a combination of sliding and rolling friction can induce further positive effects on friction and wear properties [24].

Different mechanisms that build a stable nanoparticle film on the disc surfaces are known. Possible explanations can be the fusing of particles with the surface, chemical reactions, and tribosintering [23]. However, for TiO_2 particles, these effects seem to play a minor role [25]. It could be more likely that the particles are simply pressed into the surface. We further investigated this aspect with X-ray photoelectron spectroscopy (XPS) on both discs after they were used in a test run with the final recipe based on T 805 particles. Both discs were prepared by thoroughly cleaning with acetone and petroleum ether for 2 min in an ultrasonic bath before inserting them into the XPS UHV chamber.

The XPS spectra in Fig. 7 demonstrate that TiO_2 could still be detected on both discs inside their running marks. Obviously, the quite aggressive cleaning procedure was not strong enough to overcome adhesion forces between nanoparticles and the surfaces. In addition, we further investigated the situation with helium ion micrographs (HIM) of the same discs used in the XPS measurements (Fig. 8). Nearly equal sized nanoparticles could be discerned on both surfaces inside the running marks. On the cast iron disc (Fig. 8, left), the mean diameter of these particles is (23.8 ± 4.9) nm ($n = 50$). On the 100Cr6 disc (Fig. 8, right), we measured (24.3 ± 5.8) nm ($n = 50$). These values lie remarkably close to the specified diameter of the T 805 particles (Table 1). In contrast, we did not find any particles on images outside the running marks. These results indicate that the observed particular structures could indeed be T805 nanoparticles bound or even implanted into the surfaces of both discs. We furthermore observed that the particles were distributed quite randomly on the cast iron discs. On the 100Cr6 discs, the particles were mainly organized in clusters near local surface disruptions but without any direct contact to each other. We speculate that the reason for this observation could be surface chemical reactions that took place on the 100Cr6 discs, while the particles were simply pressed into the softer cast iron discs. However, their density is obviously too low to provide sufficient tribological activity. Nevertheless, one has to keep in mind that the surfaces were thoroughly cleaned with aggressive solvents in an ultrasonic bath to be able to insert the samples into an UHV recipient. This process could have removed considerable amounts of nanoparticles from the surface before images or spectra were taken. The actual particle concentration on the surface could thus be much higher during the friction analysis. From the narrow size distribution, we furthermore conclude that most of the particles will stay intact during a test run while particle disruptions are negligible.

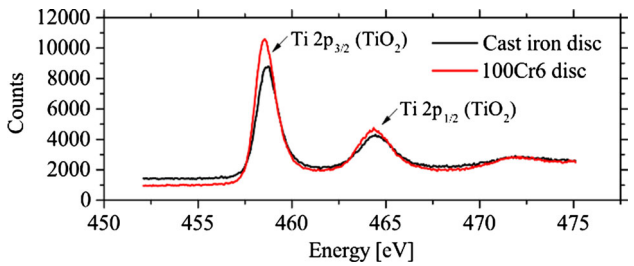

Fig. 7 Material analysis with X-ray photoelectron spectroscopy inside the running marks of a 100Cr6 and a cast iron disc after a disc–disc test run with food-tech-oil, 1 wt% T805 particles, 0.5 wt% Estisol® 242, 0.15 wt% oleylamine, and 0.15 wt% Pluronic® RPE 2520. Titanium dioxide could be detected on both disc surfaces even after cleaning them with a 1:1 mixture of petroleum ether and acetone in an ultrasonic bath for 2 min. The same discs were imaged in Fig. 8 (Color figure online)

In order to characterize wear in these experiments, we inspected optical micrographs of the running marks after the experiments with 1 wt% oleic acid (Fig. 9 top) and with 1 wt% oleic acid and 0.2 wt% T 805 particles (Fig. 9 bottom). First, both additives significantly reduced wear compared to our base oil (Fig. 4) on both materials. There are especially no significant surface disruptions observable. Merely, a soft smoothing of the active surfaces is visible. One can conclude from Fig. 9a and c that this smoothing effect is stronger, when only 1 wt% oleic acid is added to the base oil as the bright slightly reflective areas are more prominent in (a) compared to (c). However, the situation is opposite, when the 100Cr6 discs are inspected. When T 805 particles are added, slight traces of wear are observable, while the other surface in (b) is barely scratched. From these findings and with the results from Fig. 7 in mind, one can conclude here that the softer cast iron surface seems to be more appropriately protected by the implanted particles.

3.2 Stabilizing the TiO_2 Particle Suspensions and Optimal Application Concentration

The previous experiments with 1 wt% oleic acid and 0.2 wt% of T 805 titanium dioxide nanoparticles in base oil exhibit significant reduction in friction and wear compared to the pure base oil. However, the produced suspensions of oil and nanoparticles are not stable concerning sedimentation and deposition of additives. For example, the use of the hydrophilic P 25 nanoparticles inevitably leads to particle sedimentation within a few hours, which is not desirable concerning an application in the field. The dispensability and shelf time of T 805 particles is better. However, even these particles sediment after roughly 24 h.

The first step to a stable suspension of nanoparticles is their effective wetting. For this purpose, we analyzed the influence of different concentrations of oleylamine as wetting agent on the sedimentation behavior of T 805 particles suspended in the base oil, 1 wt% Estisol® 242, and 0.15 wt% Pluronic® RPE 2520 (Fig. 10a–e). Without oleylamine, the T 805 nanoparticles sediment only after 24 h (Fig. 10a). With oleylamine added, the particles are still well suspended after 5 months (Fig. 10b–e). The optimum concentration seems to be 0.15 wt% (Fig. 10c). With less oleylamine, the particles still tend to sediment. With higher concentrations, buoyancy overweighs. For steric stabilization of the suspension, we tried different concentrations of the block copolymer Pluronic® RPE2520 (Fig. 10f–j). In suspension without this agent, but with 0.15 wt% oleylamine, the nanoparticles tend to sediment after 3 months (Fig. 10f). Increasing concentrations of Pluronic® RPE 2520 result in more stable suspensions after 8 months. From Fig. 10h and i, one can conclude that

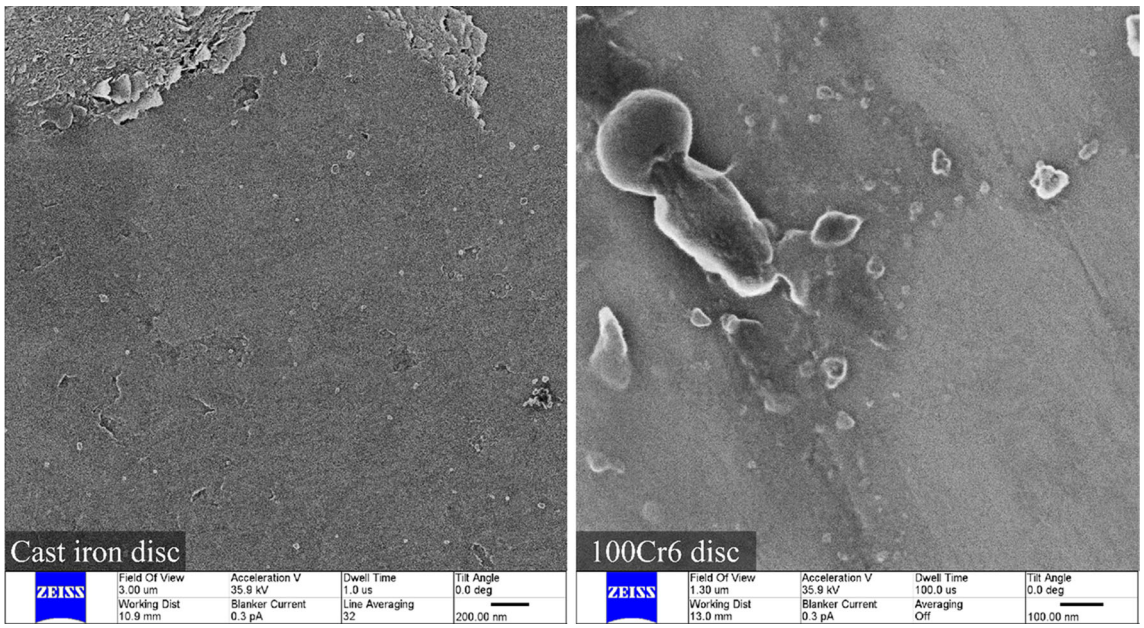

Fig. 8 Helium ion micrographs (Zeiss Orion Plus) of the running marks on the cast iron disc (*left*) and the 100Cr6 disc (*right*) from Fig. 7. Nearly equal sized particles with similar shape could be detected on both surfaces with a mean diameter of (23.8 ± 4.9) nm ($n = 50$ for cast iron) and (24.3 ± 5.8) nm ($n = 50$ for 100Cr6). According to the datasheet, T 805 particles have a mean diameter of 20 nm, which lies well within the error margins of the obtained values. For better visibility, image contrast was slightly increased using GIMP (Color figure online)

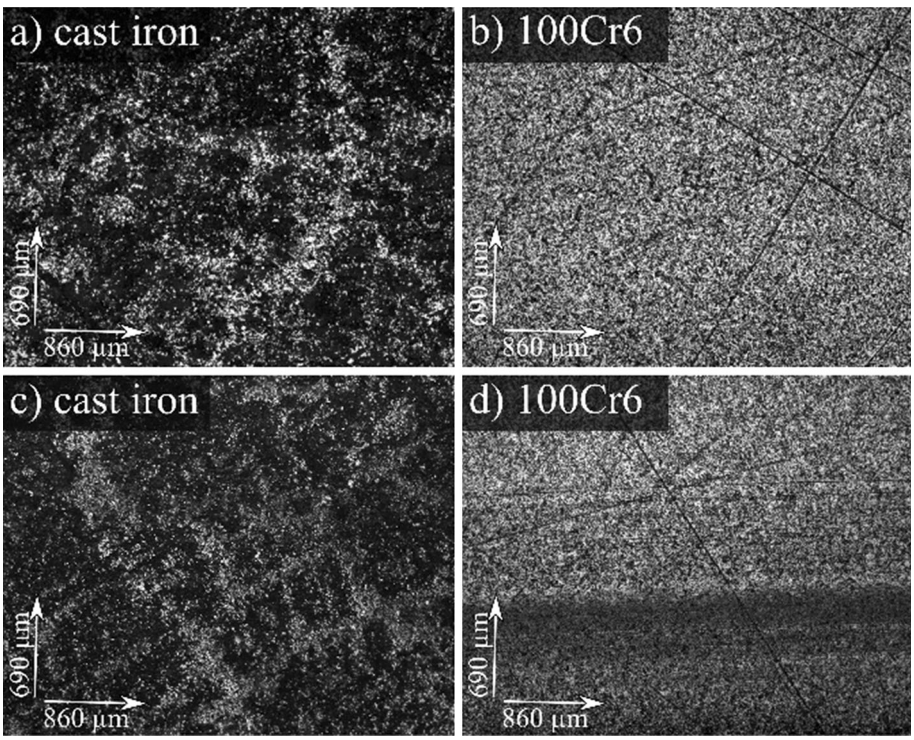

Fig. 9 Optical micrographs showing running marks on (**a**), (**b**) a disc–disc contact used in a triboexperiment with food-tech-oil and 1 wt% oleic acid and (**c**), (**d**) a pair of discs used in an experiment with food tech oil, 1 wt% oleic acid and 0.2 wt% T 805 particles

concentrations between 0.15 and 0.3 wt% perform best. We thus chose a working concentration of 0.15 wt% oleylamine and 0.15 wt% Pluronic® RPE 2520 for the following experiments or 15 wt% in relation to the amount of nanoparticles, respectively. To control the viscosity of the suspension, we furthermore added the fatty acid ester

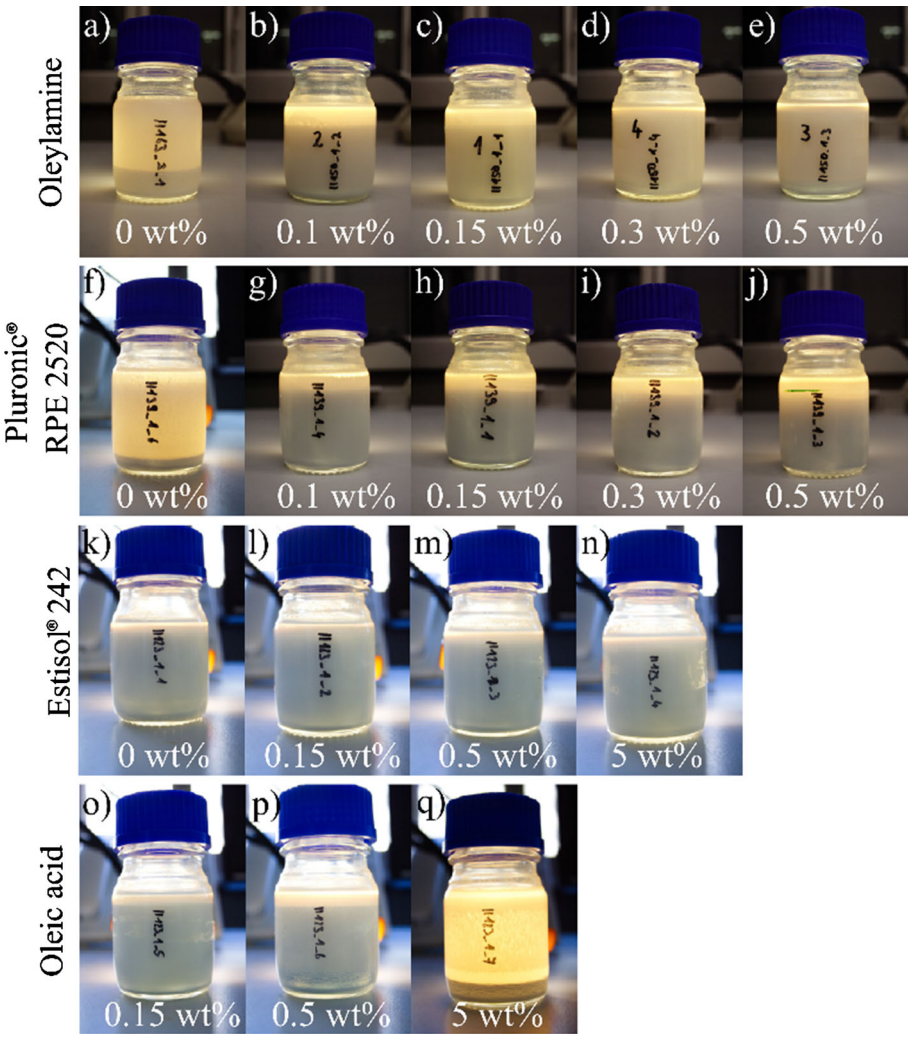

Fig. 10 Analysis of T 805 nanoparticle suspension stability. *First row*: analysis in dependence of the oleylamine concentration as wetting agent (**a**) after 24 h, **b–e** after 5 months. All samples contain 1 wt% T 805, 1 wt% Estisol® 242, and 0.15 wt% Pluronic® RPE 2520. *Second row*: analysis in dependence of the Pluronic® RPE 2520 concentration as steric stabilization agent **f** after 3 months, **g–j** after 8 months. All samples contain 1 wt% T 805, 1 wt% Estisol® 242, and 0.15 wt% oleylamine. *Third row*: analysis in dependence of the Estisol® 242 concentration **k–m** after 5 months. All samples contain 1 wt% T 805, 0.15 wt% Pluronic RPE 2520 and 0.15 wt% oleylamine. Fourth row: analysis in dependence of the oleic acid concentration **o–q** after 5 months. All samples contain 1 wt% T 805, 0.15 wt% Pluronic RPE 2520 and 0.15 wt% oleylamine. Note that all suspensions were dispersed with ultrasound for 2 min in advance and then stored for the indicated period (Color figure online)

Estisol® 242. This chemical has a quite low dynamic viscosity ($\eta_{20\ °C} = 3.9$ m Pa s) and is used to stabilize the viscosity of our suspension, when the particle concentration and thus the polymer concentration rise. Figure 10k–n shows that the addition of Estisol® 242 has no notable influence on the suspension stability. Thus, in the following, 1 wt% of Estisol® 242 is used.

The previous friction experiments showed a synergetic effect between the nanoparticles and the oleic acid (Fig. 6). This chemical however is not involved in a successful stable dispersion of the nanoparticles. Nevertheless, we investigated its possible influence on the just discussed stabilization of our nanoparticles in the base oil as well (Fig. 10o–q). It is clearly observable after 5 months that increasing the concentration of oleic acid is counterproductive. Adding 5 wt% of oleic acid causes efficient sedimentation (Fig. 10q), while this trend is rather small for lower concentrations (Fig. 10o–p) so that the previously suggested addition of oleic acid is acceptable. In conclusion and with reference to the particle concentration, the solution is well stabilized and shows good anti-friction performance with the following additives with respect to the amount of particles: 15 wt% oleylamine, 15 wt% Pluronic® 2520, and 100 wt% Estisol® 242 instead of oleic acid.

In addition, we investigated the optimal particle concentration for maximum lubrication performance with minimal costs. Figure 11 demonstrates that a concentration of 0.2 wt% T 805 particles is just sufficient to minimize friction while a minimum amount of particles and further additives is required. Further increase in the particle concentration does not lead to further increased anti-friction performance of our lubricant. However, in this concentration regime, the dynamic viscosity of the formulated lubricants is constant between 0 and 1 wt% T 805 and then slowly increases (see Fig. 3 of the supplementary information). With the results from Fig. 11 in mind, we can thus conclude once more that the actual working regime of our experiments lies well within the mixed friction regime with very low contribution from liquid friction and that a change

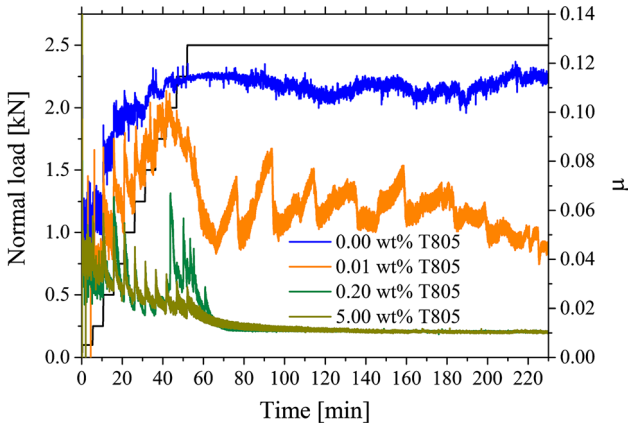

Fig. 11 Friction coefficients in dependence of different concentrations of T 805 nanoparticles with 15 wt% oleylamine and 15 wt% Pluronic® RPE 2520 with reference to the particle concentration. The Estisol 242 concentration is equal to the particle concentration with the exception of the 5 wt% T 805 run, where 2.5 wt% Estisol® 242 was added (Color figure online)

in viscosity due to addition of particles is not the governing physical principle behind our reduction of friction.

These findings are consistent with the microscopic analysis of the involved discs before and after the experiment with different concentrations of nanoparticles and additives (Fig. 12). A comparison of the used discs with the freshly lapped one in the upper left image shows the smallest amount of wear at concentrations between 0.5 and 1 wt% T 805 particles for the 100Cr6 discs. Higher concentrations lead to an increased smoothing of the discs, which can be identified by considering the increasing number of bright reflecting areas in the micrograph. Lower concentrations led to significant abrasive wear. The wear marks on the cast iron discs are even more prominent. Severe damages can be identified for concentrations lower than 0.01 wt%. Adding 0.01 wt% T 805 particles is barely sufficient to reduce wear. Optimum concentrations can be identified between 0.1 and 1 wt%. Higher concentrations lead to smoothing of the discs here as well.

In conclusion, our proposed lubricant is based on food-tech-oil, a highly purified paraffin oil, 0.5–1 wt% Aeroxide® T 805 TiO_2 nanoparticles, 15 wt% oleylamine, 15 wt% Pluronic® RPE 2520, and 100 wt% Estisol® 242 (all liquid additive concentrations are referenced to the nanoparticle concentration).

3.3 Wear Analysis with a Disc–Ball Contact

Although qualitatively observable in the previously shown micrographs, the total rate of material lost by wear cannot be measured with this setup as wear rates lie below the detection regime of the touch probe sensor in the disc–disc experiments. To evaluate the anti-wear performance of our lubricant quantitatively and under even more extreme conditions, we take additional disc–ball measurements with the same lubrication formulation. The measured friction coefficients (Fig. 13a) range from approximately 0.07–0.09 and are much more indistinguishable than in the disc–disc

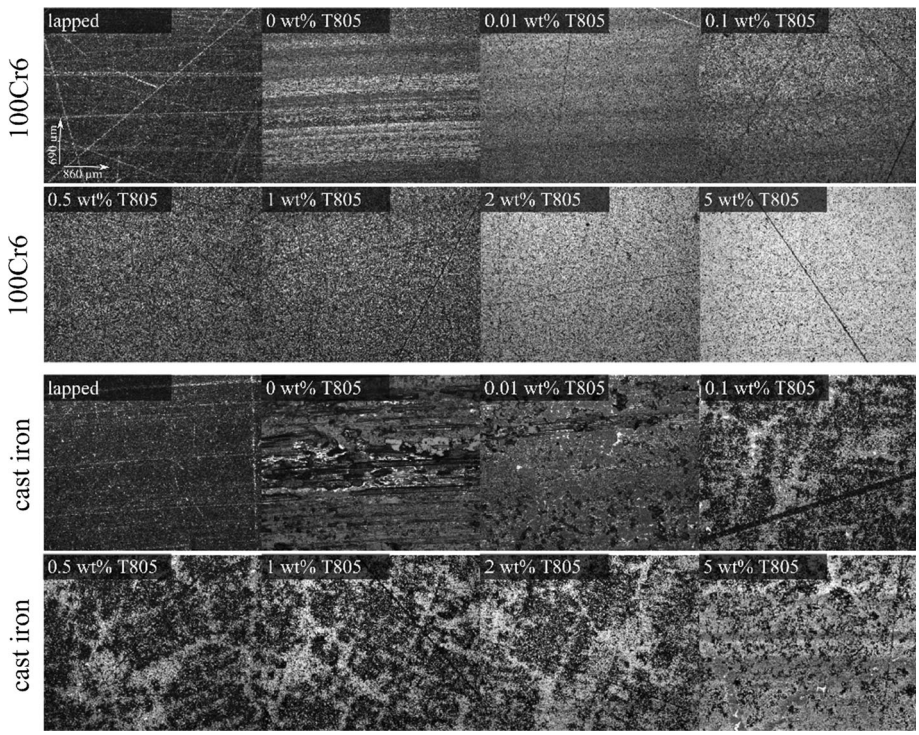

Fig. 12 Micrographs of the discs involved in experiments to find the optimal concentration of TiO_2 particles in the base oil. The least amount of wear was found for 0.5 wt% T 805 and 1 wt% T 805 on the 100Cr6 discs and for 0.1–1 wt% T 805 for the cast iron discs

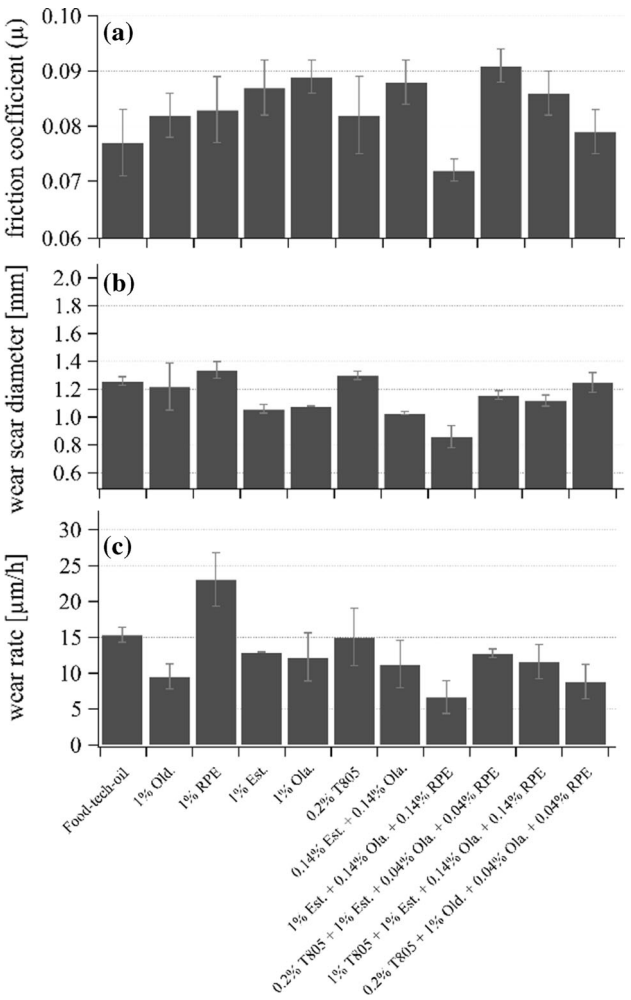

Fig. 13 Analysis of friction coefficients (**a**), wear scar diameters (**b**), and wear rates (**c**) in disc–ball measurements in dependence of the employed lubricant formulation. For better readability, we introduced the following abbreviations: Old. = oleic acid, RPE = Pluronic® RPE 2520, Est. = Estisol® 242, Ola. = oleylamine. To produce the figure, at least two datasets per lubricant were averaged, and the standard deviation was calculated. Friction coefficients and wear rates were measured only during the last hour of a certain test run to avoid the start-up phase. All wear rates are corrected for temperature expansion errors with an empirically quantified thermal expansion coefficient of (3.1923 ± 0.024) μm/K in our system

experiments. In this friction regime, the best performing formulation consists of only the dispersing additives Estisol® 242, Oleylamine, and Pluronic® RPE 2520, while the pure base oil and mixtures containing nanoparticles perform worse. However, the more accurate method of characterizing tribological properties in the border friction regime is wear rates, which are expressed here in terms of the wear scar diameters on the 100Cr6 balls quantified via optical microscopy (Fig. 13b). The smallest wear scars were obtained with the formulation that also demonstrated the smallest friction coefficients in Fig. 13a. On the other hand, the pure base oil showed rather disadvantageous wear properties compared to its performance in lowering the friction coefficient. In particular, its wear scars are larger or comparable to mixtures containing nanoparticles.

Using the integrated touch probe sensor of our tribometer, we gained access to explicit wear rates in the disc–ball system with *excluded* start-up phase (Fig. 13c). This exclusion is of course not possible with wear scar analyses. To compensate for thermal expansion effects, we introduced an empirically quantified thermal expansion coefficient. After an experiment, we let the system cool down from 60 °C to room temperature and recorded touch probe data. The resulting thermal expansion coefficient for our specific system is $\alpha = 3.1923 \pm 0.024$ μm/K which is subtracted in all our measurements. The wear rate is subsequently obtained by fitting a linear function to the last hour of each wear dataset. The start-up phase is thus not considered. Again, at least two results were averaged to generate Fig. 13c. In most instances, these results are consistent with the wear scar data in Fig. 13b. The sample containing Estisol® 242, Oleylamine, and Pluronic® RPE 2520 is again best performing. Most of the formulations containing nanoparticles exhibit lower wear rates than the base oil alone. However, some test runs (e.g., 1 wt% Pluronic® RPE 2520) reveal that the start-up phase (which is not included in Fig. 13c) can have a significant positive and also negative influence on the finally measured wear scars as wear scar and wear rate data are sometimes not consistent.

Figure 14 shows a closer representative analysis of the wear marks on the disc surfaces. The worst wear damages are clearly observable when using the plain base oil (Fig. 14a). The mixture containing only the liquid additives but no TiO_2 nanoparticles still leads to significant abrasive and adhesive wear, although it performed best in the previous analysis of the balls (Fig. 14b). On the disc, the fully formulated mixture consisting of 1 wt% T 805 particles and the liquid additives (1 wt% Estisol® 242, 0.15 wt% oleylamine, and 0.15 wt% Pluronic® RPE 2520) provides the best anti-wear performance (Fig. 14c). Only minor disc smoothing is observable.

Although the results from Figs. 13 and 14 seem contradictory to each other, a closer inspection might reveal different modes of wear on both tribopartners. During the test runs, the active tribological surface of the 100Cr6 balls is always in contact with the disc.

The engagement ratio

$$\varepsilon = \frac{\text{tribocontact area}}{\text{whole active surface area}}$$

is consequently $\varepsilon = 1$ in this case. However, for the 100Cr6 discs, ε is much smaller than 1 because only a small part of the tribologically active surface is in contact with the discs. This opens up the possibility that chemical

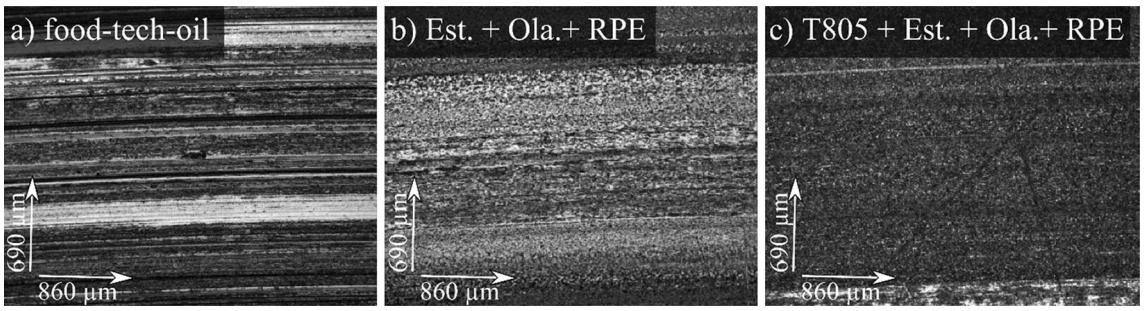

Fig. 14 Micrographs of the 100Cr6 discs after disc–ball experiments. For better readability, the abbreviations Est. = 1 wt% Estisol® 242, Ola. = 0.15 wt% oleylamine, RPE = 0.15 wt% Pluronic® RPE 2520 were used

wear modifying layers are established on the disc surface on all those parts that are not in contact with the ball. Such layers can, e.g., be formed by our liquid additives, which bind to the metal surface via physisorption. In contrast, the ball surface, which is always in contact with the discs, cannot effectively benefit from physisorption of additives. When nanoparticles are introduced, wear is shifted from the disc surface to the ball (compare Figs. 14c and 13). The reason for this observation could be that the nanoparticles bind to the physisorbed chemical layer on the disc surface or even get integrated or implanted into the layer. In conclusion, the observed shift of wear from the disc surface to the ball could be a hint for a synergetic relationship between the additives and the nanoparticles.

4 Conclusions

In this work, we investigated the anti-friction and anti-wear performance of nanoparticle supplemented paraffin oil with further chemical dispersing and stabilizing additives. Using disc–disc and disc–ball contacts, we demonstrated that especially Aerosil® T 805 TiO_2 nanoparticles showed excellent tribological properties. In contrast, silicon dioxide nanoparticles performed significantly worse. The disc–disc contact consisted of a 100Cr6 disc and a segmented cast iron disc. In 4-h test runs with a normal pressure of 10 MPa and 0.15 m/s sliding velocity, the addition of 0.5–1 wt% T 805 particles, 1 wt% Estisol® 242, 0.15 wt% oleylamine, and 0.15 wt% Pluronic® RPE 2520 to the base oil was sufficient to significantly reduce friction roughly 12-fold compared to the plain base oil. Optical micrographs of the probed discs exhibited significantly reduced wear on the disc surfaces after the experiments as well. XPS spectra and helium ion micrographs of both discs revealed that titanium dioxide nanoparticles were pressed into both discs. While the disc–disc contact operated in the mixed friction regime, the properties of our developed formulations were tested in the border friction regime as well using a disc–ball contact made of 100Cr6. We found that especially the discs were well protected by tribochemical layers that formed during the test runs and showed significantly reduced wear compared to the plain base oil. Possible applications of the developed formulation could be the reduction in friction and wear in environments, where conventional wear reducing additives do not build tribochemical surface protecting layers due to too low temperatures or where temperatures are too high for conventional friction modifiers. Applications in systems with a steady back-and-forth movement such as bed tracks are considerable as well. Here, a conventional hydrodynamic lubricating film could break down when changing the sliding direction, in contrast to a nano-supplemented film.

Acknowledgments We acknowledge Bio-Circle surface technology GmbH, Gütersloh, Germany, for providing the tribometer and many test chemicals, Evonik Industries for providing nanoparticles, the German Federal Ministry for Economic Affairs and Energy for funding this work within the ZIM initiative, and Paul Penner for providing XPS measurements.

Conflict of interest The authors declare that they have no conflict of interest.

References

1. Peng, D.X., Kang, Y., Hwang, R.M., Shyr, S.S., Chang, Y.P.: Tribological properties of diamond and SiO_2 nanoparticles added in paraffin. Tribol. Int. **42**, 911–917 (2009)
2. Li, X., Cao, Z., Zhang, Z., Dang, H.: Surface-modification in situ of nano-SiO_2 and its structure and tribological properties. Appl. Surf. Sci. **252**, 7856–7861 (2006)
3. Hu, Z.S., Dong, J.X., Chen, G.X., He, J.Z.: Preparation and tribological properties of nanoparticle lanthanum borate. Wear **243**, 43–47 (2000)
4. Battez, A.H., González, R., Viesca, J.L., Fernández, J.E., Díaz Fernández, J.M., Machado, A., Chou, R., Riba, J.: CuO, ZrO2 and ZnO nanoparticles as antiwear additive in oil lubricants. Wear **265**, 422–428 (2008)
5. Zhou, J., Wu, Z., Zhang, Z., Liu, W., Xue, Q.: Tribological behavior and lubricating mechanism of Cu nanoparticles in oil. Tribol. Lett. **8**, 213–218 (2000)

6. Padgurskas, J., Rukuiza, R., Prosyčevas, I., Kreivaitis, R.: Tribological properties of lubricant additives of Fe, Cu and Co nanoparticles. Tribol. Int. **60**, 224–232 (2013)
7. Viesca, J.L., Battez, A.H., González, R., Chou, R., Cabello, J.J.: Antiwear properties of carbon-coated copper nanoparticles used as an additive to a polyalphaolefin. Tribol. Int. **44**, 829–833 (2011)
8. Zhang, M., Wang, X., Fu, X., Xia, Y.: Performance and anti-wear mechanism of $CaCO_3$ nanoparticles as a green additive in poly-alpha-olefin. Tribol. Int. **42**, 1029–1039 (2009)
9. Chen, S., Liu, W., Yu, L.: Preparation of DDP-coated PbS nanoparticles and investigation of the antiwear ability of the prepared nanoparticles as additive in liquid paraffin. Wear **218**, 153–158 (1998)
10. Shenoy, B.S., Binu, K.G., Pai, R., Rao, D.S., Pai, R.S.: Effect of nanoparticles additives on the performance of an externally adjustable fluid film bearing. Tribol. Int. **45**, 38–42 (2012)
11. Xue, Q., Liu, W., Zhang, Z.: Friction and wear properties of a surface-modified TiO2 nanoparticle as an additive in liquid paraffin. Wear **213**, 29–32 (1997)
12. Ye, W., Cheng, T., Ye, Q., Guo, X., Zhang, Z., Dang, H.: Preparation and tribological properties of tetrafluorobenzoic acid-modified TiO2 nanoparticles as lubricant additives. Mater. Sci. Eng., A **359**, 82–85 (2003)
13. Rapoport, L., Bilik, Y., Feldman, Y., Homyonfer, M., Cohen, S.R., Tenne, R.: Hollow nanoparticles of WS2 as potential solid-state lubricants. Nature **387**, 791–793 (1997)
14. Rapoport, L., Feldman, Y., Homyonfer, M., Cohen, H., Sloan, J., Hutchison, J.L., Tenne, R.: Inorganic fullerene-like material as additives to lubricants: structure–function relationship. Wear **225–229**, 975–982 (1999)
15. Tenne, R., Homyonfer, M., Feldman, Y.: Nanoparticles of layered compounds with hollow cage structures (inorganic fullerene-like structures). Chem. Mater. **10**, 3225–3238 (1998)
16. Lee, K., Hwang, Y., Cheong, S., Choi, Y., Kwon, L., Lee, J., Kim, S.H.: Understanding the role of nanoparticles in nano-oil lubrication. Tribol. Lett. **35**, 127–131 (2009)
17. So, H., Chen, C.H.: Effects of micro-wedges formed between parallel surfaces on mixed lubrication—part I: experimental evidence. Tribol. Lett. **17**, 513–520 (2004)
18. Mate, C.M.: Tribology on the small scale. A bottom up approach to friction, lubrication, and wear. Mesoscopic physics and nanotechnology, vol. 6. Oxford University Press, Oxford (2008)
19. Grote, K.-H., Antonsson, E.K.: Springer handbook of mechanical engineering. Springer, Berlin (2009)
20. Hsu, S.M., Klaus, E.E.: Some chemical effects in boundary lubrication part I: base oil-metal interaction. ASLE Trans. **22**, 135–145 (1979)
21. Zhang, L., Chen, L., Wan, H., Chen, J., Zhou, H.: Synthesis and tribological properties of stearic acid-modified anatase (TiO2) nanoparticles. Tribol. Lett. **41**, 409–416 (2011)
22. Gao, Y., Sun, R., Zhang, Z., Xue, Q.: Tribological properties of oleic acid—modified TiO2 nanoparticle in water. Mater. Sci. Eng., A **286**, 149–151 (2000)
23. Battez, A.H., González, R., Felgueroso, D., Fernández, J.E., del Rocío, M., García, M.A., Peñuelas, I.: Wear prevention behaviour of nanoparticle suspension under extreme pressure conditions. Wear **263**, 1568–1574 (2007)
24. Tao, X., Jiazheng, Z., Kang, X.: The ball-bearing effect of diamond nanoparticles as an oil additive. J. Phys. D Appl. Phys. **29**, 2932–2937 (1996)
25. Kato, H., Komai, K.: Tribofilm formation and mild wear by tribosintering of nanometer-sized oxide particles on rubbing steel surfaces. Wear **262**, 36–41 (2007)